Hindawi
International Journal of Antennas and Propagation
Volume 2022, Article ID 1114234, 10 pages
https://doi.org/10.1155/2022/1114234

Research Article

A Method to Improve the Performance of Arrays for Aperture-Level Simultaneous Transmit and Receive

Dujuan Hu,[1] **Xizhang Wei**,[2] **Mingcong Xie**,[2] **and Yanqun Tang**[2]

[1]*School of Systems Science and Engineering, Sun Yat-Sen University, Guangzhou 528406, China*
[2]*School of Electronics and Communication Engineering, Sun Yat-Sen University, Shenzhen 518107, China*

Correspondence should be addressed to Xizhang Wei; weixzh7@mail.sysu.edu.cn

Received 30 March 2022; Revised 29 May 2022; Accepted 16 June 2022; Published 18 July 2022

Academic Editor: Stefano Selleri

The simultaneous transmit and receive (STAR) system needs to establish sufficiently high isolation between the transmitter and the receiver in order to play its role. However, due to the nonlinear characteristics and the accompanying noise of the active devices in the system, the coupling from the transmit channel to the receive channel cannot be accurately estimated in massive arrays, making it hard to improve the isolation between the transmit and receive channels. This paper proposes a new method to enhance isolation for aperture-level transmitting array and receiving array. The method uses the transmit and receive beamforming technology and aperture optimization technology to enhance the isolation between the transmitting aperture and the receiving aperture. The experimental results show that when the transmit power of an 8-element Vivaldi array is 30 W, the effective isotropic isolation (EII) peak value reaches 153.9 dB. The noise floor of the system is −89.9 dBm. Compared to only using aperture optimization and only using beamforming technology, the scheme in this paper, respectively, improves the isolation of 20.69 and 6.17 dB.

1. Introduction

The operating system of the traditional phased array is usually a time division duplex, which takes up more time resources and reduces phased array efficiency. In order to alleviate this problem, the simultaneous transmit and receive (STAR) technology was proposed [1] and attracted great attention in communications, radar, spectral sensing, and military radio [2, 3]. STAR sustains radio devices to transmit (TX) and receive (RX) at the same frequency band simultaneously, thereby improving throughput and spectrum efficiency in wireless communication systems. STAR technology was also used in continuous-wave radar to achieve stealth by continuously emitting low-power waveforms to continuously illuminate the target [4]. More recently, military radio had called STAR technology a disruptive technology that has the potential to bring about a paradigm shift in operating on the networked electromagnetic battlefield [5]. However, the premise of the successful application of STAR is how to reduce the interference and noise present in the received signal due to colocated transmitters.

Researchers had carried out many studies to enhance the isolation between the transmit and receive of a digital phased array. A digital-controlled method, called Soft Null, was presented and studied to enable full-duplex in many-antenna systems. In the case of a 72-element array partitioned as 36 transmitting antennas and 36 receiving antennas, 50 dB of preanalog self-interference cancellation (SIC) was achieved using beamforming technology while sacrificing only 12 of the 36 available transit dimensions [6]. Zhang et al. [7] expected to model the coupling path characteristics of all spatial links between the transmitting aperture and receiving aperture and used digital beamforming and digital self-interference cancellation techniques to study the cancellation performance between the transmitting aperture and different receive position array elements [8]. However, the effect of the transmit and receive aperture shapes on isolation was not explored. The MIT team divided all

transmitting subarray in a phased array into transmitting apertures, and all receiving subarray into receiving apertures, which was termed aperture-level simultaneous transmit and receive (ALSTAR) [9]. They attempted to improve the isolation between transmit and receive apertures using a new digital cancellation structure and beamforming techniques. In terms of the design of the transmit and receive apertures, they drew schematic diagrams of two different transmit and receive apertures but only studied the isolation in this configuration with transmit aperture on the left and receive aperture on the right. Their results showed that 163.9 dB isolation on the phased array with 25 transmitting elements and 25 receiving elements was implemented. In 2020, they further improved the theoretical study of the ALSTAR array [10]. Theoretical results suggest that the isolation could reach 187.1 dB under the condition of 2500 W transmit power between 25 transmitting elements and 25 receiving elements, while the noise floor only increased by 2.2 dB. Reference [11] proposed a broadband full-duplex phased array system with combined transmit and receive beamforming, without the need for RF cancellation links, and achieved self-interference cancellation using beamforming with minimal gain loss. In the model of the ALSTAR array, the isolation depends on key factors including transmit signal, transmit noise, coupling matrix, receive noise, and array manifold. However, existing STAR technologies focus primarily on improving isolation using beamforming and digital cancellation techniques, with little focus on the impact of array prevalence on isolation. By derivation of the equation for isolation, we find that the isolation is directly related to the shape of the transmit and receive apertures (array manifold vector). Inspired by this thought, this paper commits to reveal in depth the influence of array manifold of transmit and receive on the isolation between transmit and receive apertures, and the beamforming technology is used to further enhance the isolation.

The problem of the aperture optimization of the transmit and receive array is similar to that of the traditional array optimization, and the difference is only the objective function. The goal of the former is to maximize the isolation between the transmit antenna array and the receive antenna array by optimizing the number and positions of the transmit antenna and the receive antenna. The latter is to optimize the number and position of antenna elements to achieve a high-performance pattern [12]. Therefore, we can refer to the idea of aperture optimization to optimize the aperture of the transmit and receive array for boost isolation.

In terms of array optimization, swarm intelligence algorithms are often used for array optimization such as Ant Colony Optimization (ACO), particle swarm optimization (PSO), genetic algorithm (GA), etc. In 2006, Universidad Carlos III de Madrid proposed the ACO as a useful alternative in the thinned array design, using the side lobe level (SLL) as the desirability parameter [13]. In 2015, in order to generate radiation patterns with reduced peak side lobe level (PSLL) in a thinned linear antenna array, [14] introduced the PSO to estimate the optimum combination of "on" and "off" elements for high possible peak SLL. In 2018, Cummings et al. proposed the information theory performance indicators of narrow-band STAR imaging arrays and divided these arrays into transmit and receive apertures through detailed testing of possible partitions and the application of GA [15, 16]. In beamforming, many studies prove successful cases of swarm intelligence algorithms optimizing beamforming to improve phased array performance, such as beamforming-based pattern synthesis [17]. Reference [18] proposed an enhanced ACO algorithm to optimize the beam pointing position, beam width, and side lobes of the antenna array, which has competitive advantages over other algorithms. In 2020, new integer coded quantified angles, based on the PSO beamforming algorithm for mmWave massive MIMO communication, could achieve almost 98% performance of the full-search beamforming [19].

In this paper, we use a hybrid GA-PSO algorithm for the optimization of the transmit and receive aperture and transmit and receive beamforming of the ALSTAR architecture to enhance isolation between the transmit and receive apertures. By comparing the schemes of aperture optimization, beamforming, aperture optimization, and beamforming, it is proved that the scheme of aperture optimization and beamforming joint optimization can bring about a 20.69 dB improvement in isolation between transmit and receive apertures.

The organization of this paper is as follows. In Section 2, the signal model and optimization model of the ALSTAR array are given. Section 3, GA and PSO algorithms are introduced for aperture optimization and beamforming optimization. Section 4 discusses and analyzes the results of array aperture optimization and beamforming optimization in the ALSTAR and verifies the competitiveness of the proposed scheme. Finally, the conclusion is provided in Section 5.

2. Aperture-Level Array Signal Model

For a massive array, we first divide the array into a transmitting array and a receiving array to analyze its signal model. The signal model is shown in Figure 1; the general idea of improving the isolation between the transmitting array and the receiving array is to obtain the reference signal from the transmitter and subtract the modulated reference signal from the receiver. The reference signal of the traditional digital cancellation is derived from the digital baseband. It does not contain the transmitted noise information, which makes it impossible to cancel the self-interference component caused by the transmitter noise. To overcome this problem, ALSTAR extracts a reference signal from the output of the power amplifier to establish a reference channel and cancels the self-interference signal at the output of the receive beamformer. It can eliminate the self-interference component caused by the transmitted signal and the transmitted noise.

In Figure 1, the symbols $x(t)$, $x_t(t)$, $s(t)$, and $x_r(t)$ are the digital baseband signal, the vector of the transmitted signal, the signal of interest (SOI), and the vector of the received signal, respectively. The parameters b_t, b_r, and b_c represent the vector of transmit beamforming, the vector of receive beamforming, and the adaptive filter, respectively.

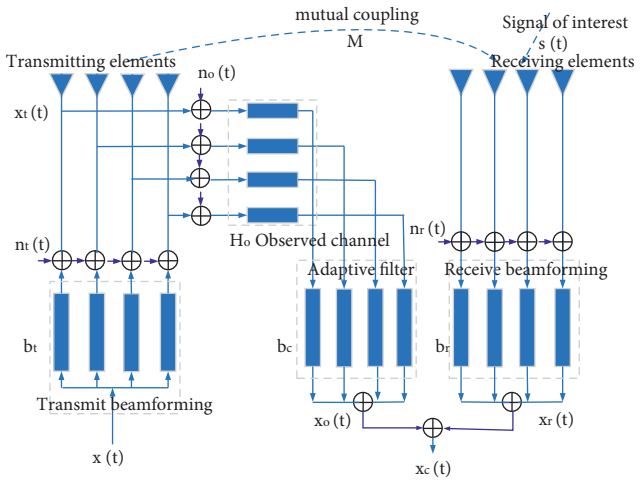

FIGURE 1: Block diagram of ALSTAR cancellation architecture.

H_o is the fixed attenuator between each transmit channel and its corresponding observation receive channel, and M is the mutual coupling channel between transmit and receive arrays. $x_o(t)$ is the observation signal. $n_t(t)$, $n_r(t)$, and $n_o(t)$ are the noise at the transmitter noise, observation channel noise, and receiver noise, respectively. $x_c(t)$ means the received signal after SIC. The signal $x_t(t)$ at the transmitting antenna can be expressed as

$$x_t(t) + b_t x(t) = n_t(t), \tag{1}$$

where $b_t = \mathbb{C}^{J\times 1}$, J is the number of the transmitting antenna, and $n_t(t)$ is zero-mean complex additive white Gaussian noise. Its covariance matrix is $N_t = E[n_t n_t^H] = \mathrm{Diag}(b_t b_t^H)/\eta_t$, where η_t is the dynamic range of the transmit channel.

The transmitted signal $x_t(t)$ couple to the receiving antennas passes through the receive channel and introduces receive noise. The signal after receive beamforming can be expressed as

$$x_r(t) = b_r[Mx_t(t) + s(t) + n_r(t)], \tag{2}$$

where $M \in \mathbb{C}^{K\times J}$, and $b_r \in \mathbb{C}^{K\times 1}$. K is the number of the receiving antennas. $n_r(t)$ is zero-mean complex Gaussian receiver noise with $N_r = E[n_r n_r^H] = \mathrm{Diag}(E[rr^H])/\eta_r + \sigma_r^2 I$. η_r is the receiver dynamic range, and σ_r^2 is the receiver thermal noise power. The expression of the reference signal after passing through the observation channel in the ALSTAR architecture can be noted as

$$x_o(t) = b_C^H[H_o(x_t(t) + n_o(t))], \tag{3}$$

where $b_c \in \mathbb{C}^{J\times 1}$. The signal $n_o(t)$ is the additive white Gaussian noise, which obeys the normal distribution $n_o(t) \sim N(0, N_O)$. N_o is equal to $\mathrm{Diag}(b_t b_t^H)/\eta_r$. The signal $x_c(t)$ after the cancellation can be expressed as

$$x_c(t) = x_r(t) - x_o(t) = b_r[n_r(t) + s(t) - Mn_o(t)]. \tag{4}$$

Obviously, the residual signals after cancellation are the receiving channel noise and the observation channel noise, as well as the signal of interest. In order to eliminate these noises as much as possible, the ALSTAR cancellation strategy replaces the larger transmitter noise with a smaller observation noise, thereby improving EII in [5]. The expression of EII is as follows:

$$EII = P_t G_r(\phi,\theta,b_r) g(\phi,\theta) \frac{b_t^H q_t(\phi,\theta) q_t^H(\phi,\theta) b_t}{b_t^H M_{bt} b_t}, \tag{5}$$

$$P_n = b_t^H M_{bt} b_t, \tag{6}$$

$$\begin{aligned} M_{bt} = {} & \eta_r^{-1}\mathrm{Diag}\left(M^H b_r b_r^H M\right) + \eta_r^{-1} M^H \mathrm{Diag}\left(b_r b_r^H\right) M \\ & + \eta_r^{-1}\eta_t^{-1}\mathrm{Diag}\left[M^H \mathrm{Diag}\left(b_r b_r^H\right) M\right] + \frac{\sigma_r^2}{P_t} I, \end{aligned} \tag{7}$$

where P_t represents the transmit power, G_r represents the total gain of the receiving array, and g is the gain of a single element. M_{bt} is the interference and noise covariance matrices, and P_n is the total residual noise in the receiver. q_t, q_r are the steering vector of the transmit and receive arrays. σ_r^2 is the thermal noise power for a 100 MHz bandwidth channel with a 3 dB noise figure. I is the unit matrix of the receiving elements, which are K rows and K columns. It can be seen that EII is not only related to the transmit and receive beamforming vectors but also related to the steering vectors of the transmit and receive arrays. That is, it is related to the arrangement of the transmitting array and the receiving array. Therefore, in order to maximize EII, the transmit and receive beamforming vector and the steering vector of the transmit and receive array should be considered optimized. Therefore, the fitness function can be defined as follows, including three constraints:

$$\begin{aligned} \text{fitness} = {} & EII_{\max_{q_{t,r}, b_{t,r}}} - \left(P_t G_r(\phi,\theta,b_r) g(\phi,\theta) \frac{b_t^H q_t(\phi,\theta) q_t^H(\phi,\theta) b_r}{b_t^H M_{bt} b_t}\right), \\ s.t. & \begin{cases} q_{t/r}(\phi,\theta) = q(\phi,\theta) p_i(\text{Iter}), \\ \|b_t\|^2 = P_t, \\ \|b_r\|^2 = 1, \end{cases} \\ EII_{\max_{q_{t,r}, b_{t,r}}} = {} & \frac{P_t J K g^2(\phi,\theta)}{\sigma_r^2}. \end{aligned} \tag{8}$$

While $q(\phi,\theta) = e^{-j(2\pi/\lambda)(x*\cos(\phi)\sin(\theta) + y*\sin(\phi)\sin(\theta))}$, x represents the distance from each element in the array plane to the x-axis, and y represents the distance from each element in the array plane to the y-axis. $p_i(\text{Iter})$ represents the transmit and receive configuration of the array element during each iteration. $EII_{\max_{q_{t,r}, b_{t,r}}}$ is the theoretical limit of the effective isotropic isolation.

3. Aperture Configuration and Beamforming

3.1. Array Aperture Partition Optimization. We know that the isolation between the transmitting antenna and the receiving antenna in different numbers and positions is inconsistent. Therefore, we need to determine the number and position of the transmit and receive antennas to get the highest isolation. For the convenience of description, we

divide all elements used for transmit into transmit apertures and all elements used for receive into receive apertures. Since each array element can be switched to be used for transmit or receive, and each array element has two possible states, we denote the transmit state and the receive state by 1 and 0, respectively. In our design, since the GA is an algorithm based on binary coding, the GA is used to optimize the working state of each antenna and then determine the transmit and receive apertures to obtain the highest isolation. First, we binary encode the states of all antennas and place them side by side to form a gene, that is, a long binary string. Each gene corresponds to a configuration for transmit and receive aperture, and the isolation between them under the transmit and receive aperture configuration can be calculated according to equations (5)–(7). Moreover, the GA has the performance of checking the number of parameter combinations, and we can use this to rule out extreme cases to reduce algorithm complexity. For a uniform linear array with N (number of array elements), its transmit and receive configuration has $2^N - 2$ cases. Here, the case of array elements representing full transmitting or full receiving is removed.

3.2. Transmit and Receive Beamforming Optimization. Before using beamforming techniques, we assume that the arrangement of the transmit and receive aperture is fixed; i.e., q_t and q_r are fixed. First of all, we use equations (5)–(7) to calculate the EII between the transmit and receive aperture and then load a random complex weight b_t and b_r from 0 to 1 on each transmit and receive antenna to implement beamforming. Since particle swarm optimization (PSO) has the characteristics of high solution accuracy and fast solution speed for nonconvex optimization problems of continuous variables, it is suitable for solving optimization problems of beamforming. In this paper, the PSO is used to find the best b_t and b_r when the isolation is the largest. Subsequently, the observation signal is modulated by the cancellation filter, and the realization method is to load a random complex weight b_c on the observation signal. Therefore, the SIC filter in the observation link can be expressed as $b_c = -b_r^H M H_o^{-1}$ under the condition of ideal cancellation, and b_c also changes with the changes of b_t and b_r. In the ALSTAR model, for any random set of transmit and receive aperture configurations, we can determine the number and location of transmit and receive array elements to maximize isolation. On this basis, we further consider the impact of beamforming on the system EII. In this paper, PSO is used to jointly optimize the transmit and receive beamforming, which is different from the traditional optimization of only optimizing transmit beamforming and only optimizing receive beamforming, and also different from the alternating optimization of 2020 MIT [10]. The advantage of this is that there is no need to construct expressions in both directions, which reduces the computational complexity.

By mimicking the foraging mechanism of birds, Eberhard and Kennedy proposed a particle swarm optimization (PSO) algorithm in 1995. In the PSO algorithm, particles represent candidate solutions, and these candidate solutions can be initialized as a matrix:

$$X = \begin{pmatrix} x_{1,1} & x_{1,2} & \cdots & x_{1,d} \\ x_{2,1} & x_{2,2} & \cdots & x_{2,d} \\ \vdots & \vdots & \ddots & \vdots \\ x_{n,1} & x_{n,2} & \cdots & x_{n,d} \end{pmatrix}, \tag{9}$$

where each row vector $[x_{i,1}, x_{i,2}, \ldots, x_{i,d}], i \in (1, 2, \ldots, n)$ represents an independent particle, n is the number of particles, and d is the number of the parameters. Generally, d can also be regarded as the dimensional number, and each particle is mapped as a set of b_t, b_r. Particles search for optimal solutions in multidimensional space by constantly changing their position and velocity vectors. In every single generation, particles update candidate solutions through velocity and position update equations. The particle velocity $v_i = [v_{i,1}, v_{i,2}, \ldots, v_{i,d}]$ and position $x_i = [x_{i,1}, x_{i,2}, \ldots, x_{i,d}]$ update equations are as follows:

$$v_i^k = \omega v_i^{k-1} + c_1 r_1 \left(P_{\text{best}} - x_i^{k-1}\right) + c_2 r_2 \left(G_{\text{best}} - x_i^{k-1}\right), \tag{10}$$

$$x_i^k = x_i^{k-1} + v_i^k. \tag{11}$$

Note that G_{best} is the global optimal of all particles in each iterative. Another important element in the PSO is local optimum P_{best}. The position change range is $[-x_{\max}, x_{\max}]$, and the speed change range is $[-v_{\max}, v_{\max}]$.

3.3. GA-PSO Hybrid Optimized Structure. The GA-PSO optimization algorithm is a hybrid algorithm that combines aperture optimization and beamforming optimization. The first is to use the GA algorithm to determine the aperture distribution. On this basis, the PSO is used to optimize the transmit and receive beamforming. Subsequently, the fitness function is used to judge whether the current aperture configuration and beamforming are optimal. Figure 2 shows the flow chart of GA-PSO for optimizing b_t, b_r and q_t, q_r. The specific process of the optimization of the aperture-level transmit and receive array based on a genetic algorithm is as follows:

(1) Initialize the number of genes according to antenna array size, initial gene configuration value, crossover probability, mutation probability, particle population, particle dimension, particle position, and velocity; the position represents parameters to be optimized b_t and b_r and the maximum number of iterations.

(2) Calculate the fitness value of each particle according to the equation (8), then the particle with the smallest fitness value is regarded as the current local optimal individual P_{best}, and the group with the smallest fitness value is regarded as the current optimal G_{best}.

(3) Perform selection, crossover, and mutation operations on genes, and obtain a new steering vector q_t, q_r according to the new gene configuration.

Selection: the selection operator is applied to the group. The purpose of selection is to inherit the optimized individuals directly to the next

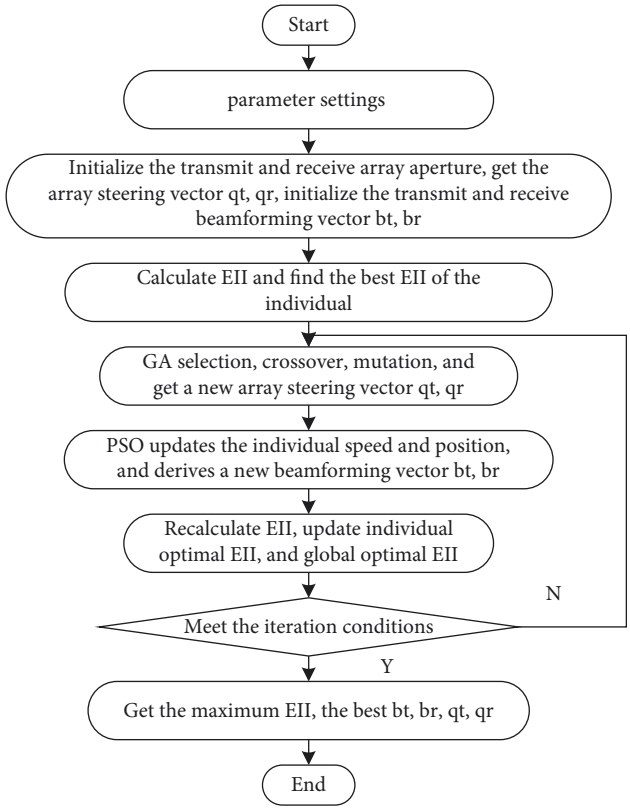

Figure 2: The flowchart of GA-PSO Hybrid optimized structure.

generation or to generate new individuals through pairing and crossover and then inherit them to the next generation. For example, if the number of array elements is 8, configuration 1 (11010101) and configuration 2 (10011011) are randomly selected as selection operators.

Cross: apply the cross operator to the group. The key role in the genetic algorithm is the crossover operator. As shown in the example in the following figure, the last three chromosomes of the selection operator are randomly crossed in pairs with a crossover probability of 0.6 to obtain a new transmit and receive configuration. For example, the last three chromosomes of the selection operator are randomly crossed in pairs to obtain a new transmit and receive configuration (11010011, 10011101).

Mutation: apply the mutation operator to the group. That is to change the gene value at some loci of the individual string in the population. Randomly select one of the two new configurations after the crossover with a mutation probability of 0.4, and mutate one of the binary numbers to obtain the latest transceiver configuration. For example, mutate one chromosome in the selected gene to get the latest transmit and receive configuration (10010101).

(4) During the k-th iteration, the position of the i-th particle x_{id}^{k} is updated using the velocity update equation (10) and the position update equation (11). Among them, the inertia weight ω changes with the number of iterations; c_1 and c_2 are, respectively, set to 2.

(5) Reevaluate the newly generated particles and recalculate their fitness values and update P_{best} and G_{best} to obtain the new b_t and b_r.

(6) If the number of iterations is greater than the maximum number of iterations, go to step (7); otherwise, go to step (3) until the termination condition is met.

(7) Obtain the optimal EII, and convert the optimal chromosome configuration of genes and the optimal position of the population into corresponding q_t, q_r and b_t, b_r.

4. Experimental Results

In order to verify the superiority of the proposed method in improving the isolation between the transmit and receive antennas, we simulated the ALSTAR model with an 8-element uniform linear array on MATLAB software. Since the EII of the ALSTAR model is directly related to the characteristics of the coupling matrix and antenna gain, it is necessary to design a phased array with high isolation and high gain. Subsequently, based on the designed phased array coupling matrix and the mode data of each element, the performance of the algorithm is discussed and analyzed.

4.1. Phased Array Design. It can be seen from equation (8) that the use of high-gain, low-coupling antenna elements helps to improve the isolation between the transmitting and the receiving arrays. In this paper, the Vivaldi antenna with high-gain and low-coupling characteristics is used as the antenna array element in the continuous-wave radar scene. The model and prototype of the phased array antenna are shown in Figure 3, and the phased array is composed of 8 Vivaldi antennas, which are arranged on a metal plate at a distance of 11 mm in turn and fed through SMA connectors. A phased array is simulated in HFSS and its results are shown in Figure 4. As can be seen, the antenna's impedance bandwidth and antenna gain are improved by slotting the antenna and microstrip-to-slot coupling feed. The working bandwidth of the antenna is 8.17–14.8 GHz, and the coupling between adjacent antennas is less than −10 in the whole bandwidth range.

The coupling matrix M is modeled to describe the state of electromagnetic waves from the transmitter to the receiver in HFSS, which is a $K \times J$ matrix, and K and J represent the number of receiving antenna and transmitting antenna. For the antenna, the coupling matrix M is actually the scattering parameter of the antenna. In the GA optimization iterative process, the array aperture partition is dynamically changing, and M also changes with the aperture partition. The position of the transmitting array element is a subset of $N = (\#1, \#2, \#3, \#4, \#5, \#6, \#7, \#8)$, denoted as $J \in N$, and the position of the receiving array element is the complement of

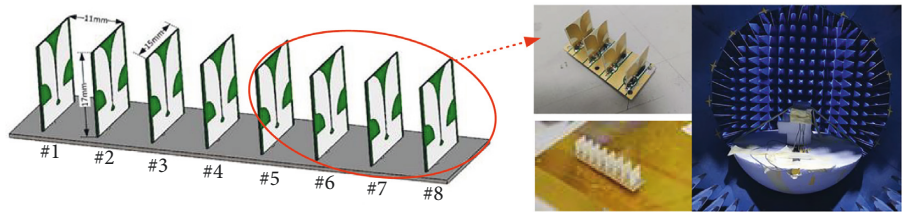

Figure 3: Model and physical prototype of phased array.

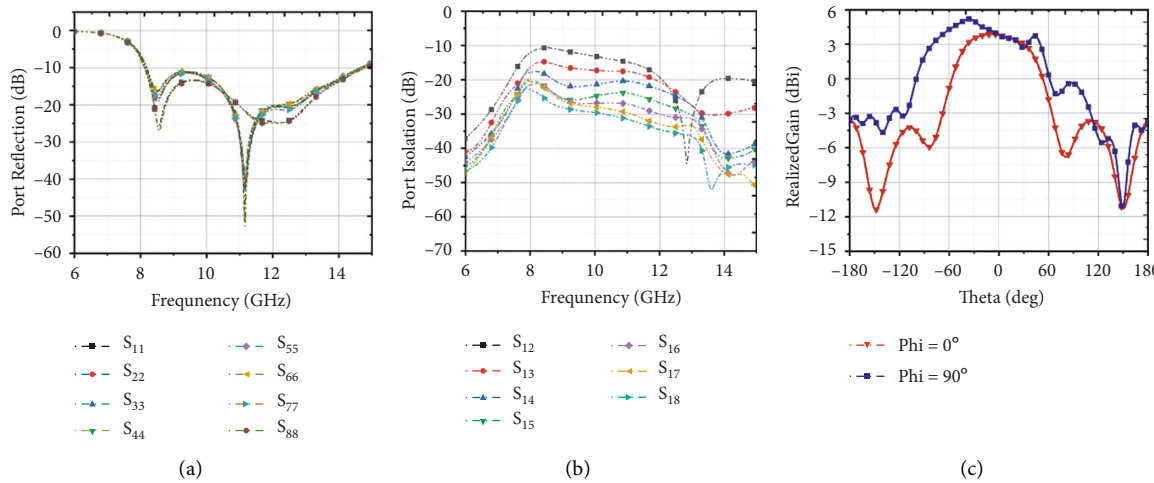

Figure 4: The performance of the phased array. (a) Port reflection coefficient curve of phased array. (b) Port isolation curve between antennas. (c) The pattern of the first antenna at 10 GHz.

$J \cup N$, denoted as $K = C_N J$. Then, the dynamically changing M is as follows:

$$
\begin{aligned}
&M = M_{K*J}, J \in N, K = C_N J, N = (1,2,3,4,5,6,7,8),\\
&\quad e.g. \left\{ \begin{array}{c} J = (2,3,7,8) \\ K = (1,4,5,6,) \end{array} \right\},\\
&\Rightarrow M = \begin{bmatrix} S_{1,2} & S_{1,3} & S_{1,7} & S_{1,8} \\ S_{4,2} & S_{4,3} & S_{4,7} & S_{4,8} \\ S_{5,2} & S_{5,3} & S_{5,7} & S_{5,8} \\ S_{6,2} & S_{6,3} & S_{6,7} & S_{6,8} \end{bmatrix},\\
&\quad e.g. \left\{ \begin{array}{c} J = (1,3,5,6,7,8) \\ K = (2,4) \end{array} \right\},\\
&\Rightarrow M = \begin{bmatrix} S_{2,1} & S_{2,3} & S_{2,5} & S_{2,6} & S_{2,7} & S_{2,8} \\ S_{4,1} & S_{4,3} & S_{4,5} & S_{4,6} & S_{4,7} & S_{4,8} \end{bmatrix}.
\end{aligned}
\tag{12}
$$

For example, the above equation gives two forms of coupling matrices, namely, the transmitting array element is #2, #3 #, #7, and #8, and the receiving array element is #1, #4, #5, and #6. And the transmitting array element is #1, #3, #5, #6, #7, and #8, and the receiving array element is #2 and #4.

4.2. Array Performance. In order to reveal the effect of the GA-PSO algorithm, we separately analyze the benefits of GA-optimized array aperture, PSO optimized beamforming, GA-PSO simultaneous optimized array aperture, and beamforming in ALSTAR. Before that, we incorporated this algorithm into the measurement and optimization model of the ALSTAR array established in equation (8). The antenna adopts the phased array designed above, and the beam scanning angle is −90° to 90°. The system's dynamic range of transmit and receive channels is set as 45 dB and 70 dB, respectively. The noise floor of the receiving channel is −91 dB, which is obtained by the 100 MHz bandwidth channel with a 3 dB noise figure. The objective function and the boundary range of the parameters are given in Section 2. The population size and number of iterations for both PSO and GA were set to 30 and 100, respectively. The experiment is duplicated 100 times independently utilizing the MATLAB software (Version: R2021a) to guarantee the reliability of the experiment results. Besides, all comparative experiments were executed on a desktop PC with an Intel Core i7-8700 CPU processor @ 3.20 GHz, 16 GB RAM, under the Windows10 64-bit OS.

Firstly, we analyze the contribution of GA to ALSTAR. As mentioned earlier, GA is used to dynamically search the receive and transmit apertures of the array to obtain the optimal transmit and receive apertures of the ALSTAR system and improve the isolation of the system. When the number of transmitting aperture antennas and the number of receiving aperture antennas are almost equal, the isolation between the transmit and receive apertures can be maximized, and the noise is minimized. Because a perfect null can be formed between the transmitting aperture and the receiving aperture only when the number of transmitting array elements is equal to the number of receiving array elements. As shown in Figure 5, when the transmit and receive

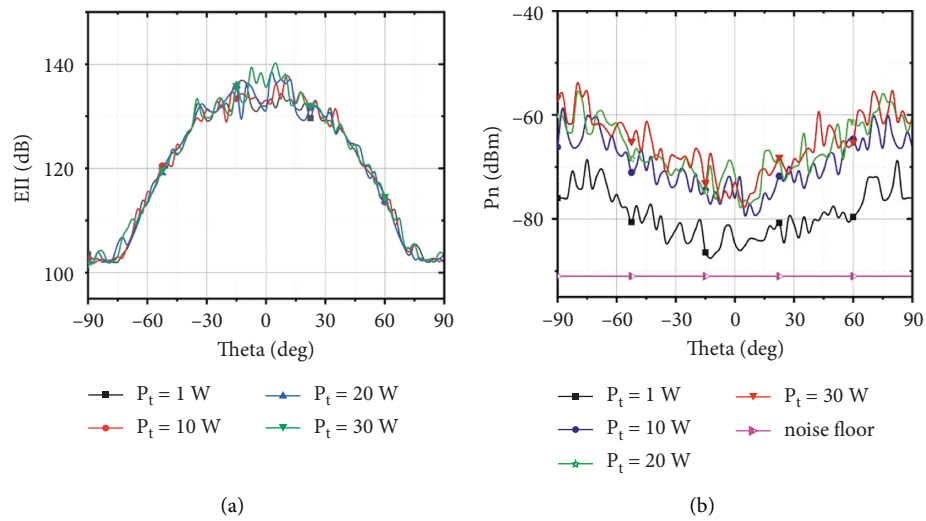

FIGURE 5: The performance of GA optimizes array partitioning at 10 GHz. (a) The EII at different transmit power. (b) The P_n at different transmit power.

apertures are configured as (00001111), that is, the transmit and receive apertures are configured as left transmit and right receive, the maximum isolation is 140.15 dB when the transmit power is 30 W and the scanning angle is 5°, and the P_n is −77.77 dBm. Further, Figure 5 also shows the isolation and noise obtained at 4 transmit powers (P_t = 1 W, 10 W, 20 W, and 30 W). When the transmit power is 1 W, the EII reaches the maximum value of 133.27 dB at 7.7° and the P_n is −87.84 dBm. When the transmit power is 10 W, the EII reaches the maximum value of 136.24 dB at 5° and the P_n is −79.26 dBm. When the transmit power is 20 W, the EII obtains the maximum value of 138.28 dB at 2.5°, and P_n is −77.66 dBm. When the transmit power is 30 W, the maximum EII is 140.15 dB at 5°, and P_n is −77.77 dBm.

Then, we analyze the influence of the PSO algorithm on the ALSTAR array. The PSO is used to optimize the ALSTAR array and study the EII under different b_t and br. The aperture partition of the array is set to 4 transmitting elements and 4 receiving elements (#1, #2, #3, and #4 are transmitting elements, and #5, #6, #7, and #8 are receiving elements). Each individual in the population is mapped to the transmit and receive beamforming weights as a feasible solution. The mapping relationship between the feasible solution and the transmit and receive beamforming weights is shown in equation (13), where there is the global optimal solution with dimensions, which contains the weights of the transmit and receive beamforming. Figure 6 shows the EII and P_n of the beamforming optimization by PSO across the scan angle for 1 W, 10 W, 20 W, and 30 W of the transmit power, respectively. We can clearly see that when the transmit power is 1 W, 10 W, 20 W, and 30 W, the values of EII at 0° are 145.89 dB, 147.79 dB, 147.93 dB, and 147.97 dB, respectively. When the transmit power is 1 W, the value of P_n at 0° is −86.85 dBm, and the value of P_n in the whole scanning angle is not a bit different. The difference between the maximum value and the minimum value is only 2.52 dBm. Moreover, with the increase of the transmit power, the EII is increasing, and the P_n is decreasing.

$$\begin{aligned} b_t &= u_t * \left(G_{\text{best}}(1\colon J) + j * G_{\text{best}}(J+1, 2J)\right), \\ b_r &= u_r * \left(G_{\text{best}}(2J+1\colon 2J+K)\right. \\ &\quad \left. + j * G_{\text{best}}(2J+K+1, 2(J+K))\right). \end{aligned} \tag{13}$$

We employed the hybrid GA-PAO to optimize the transmit and receive apertures and beamforming, which are q_t , q_r and b_t, b_r. The EII and P_n of joint optimization of array aperture and beamforming by GA-PSO across the scan space for P_t = 1 W, 10 W, 20 W, and 30 W. As shown in Figure 7, when the transmit power is 30 W, EII achieves good results of 153.87 dB and 153.96 dB at 0° and 2.5°, and the corresponding values of P_n are −89.9 dBm and −90.1 dBm, respectively. With a transmit power of 30 W and only aperture partitioning, the minimum value of P_n is −77.7 dBm, and with only beamforming optimization, the minimum value of P_n is −79.6 dBm. However, using by joint optimization, the maximum value of P_n is 90.1 dBm. Compared with the former two, the improvement is 12.4 dBm and 10.5 dBm, respectively, indicating that the GA-PSO joint optimization scheme proposed in this paper is more competitive in the design of ALSTAR arrays.

To reveal the reason why the GA-PSO algorithm improves the isolation of the ALSTAR array, we compare the performance of three methods for ALSTAR aperture optimization. Figure 8 shows the EII and P_n for array aperture partition optimization by GA, beamforming optimization by PSO, and joint optimization of array aperture partitioning and beamforming by GA-PSO. The result of the three methods is only shown for P_t = 30 W as increasing the transmitted power does not significantly change the EII of the array aperture optimization. For 0° at broadside with GA-PAO joint optimization of array aperture partitioning and beamforming, a maximum EII of 153.8 dB is accomplished. Compared with using GA to optimize transmit and receive aperture and PSO to optimize beamforming, EII improves by 18.4 dB and 5.9 dB, respectively. In addition, the P_n values are presented in Figure 8(b). It can be seen that

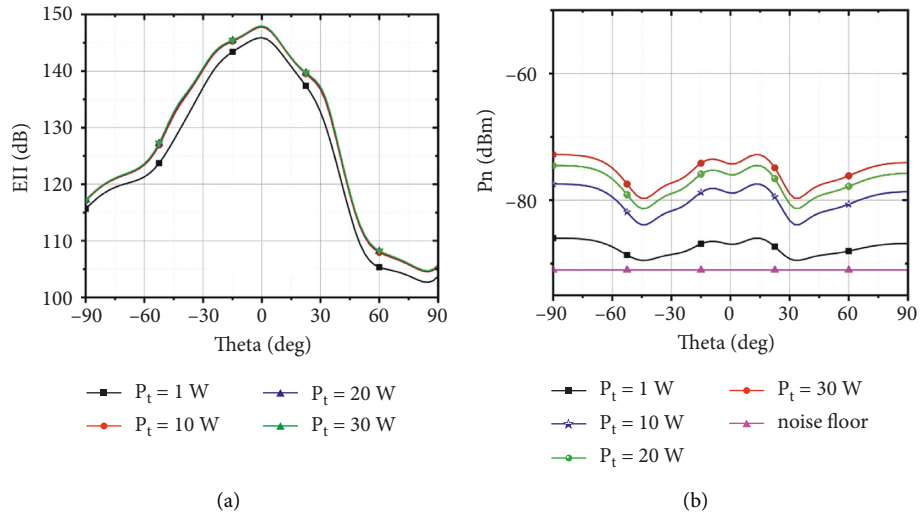

Figure 6: The performance of PSO optimizes beamforming at 10 GHz. (a) The EII at different transmit power. (b) The P_n at different transmit power.

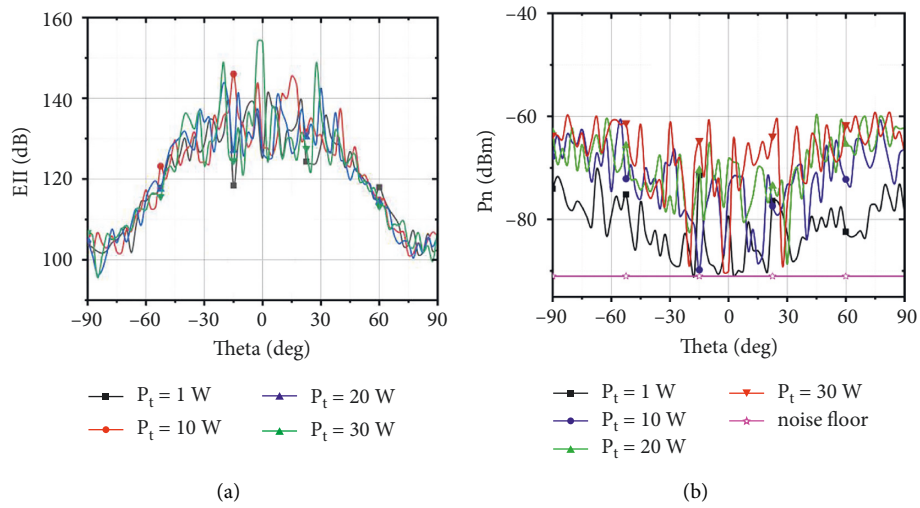

Figure 7: The performance of GA-PSO optimizes array partitioning and beamforming at 10 GHz. (a) The EII at different transmit power. (b) The P_n at different transmit power.

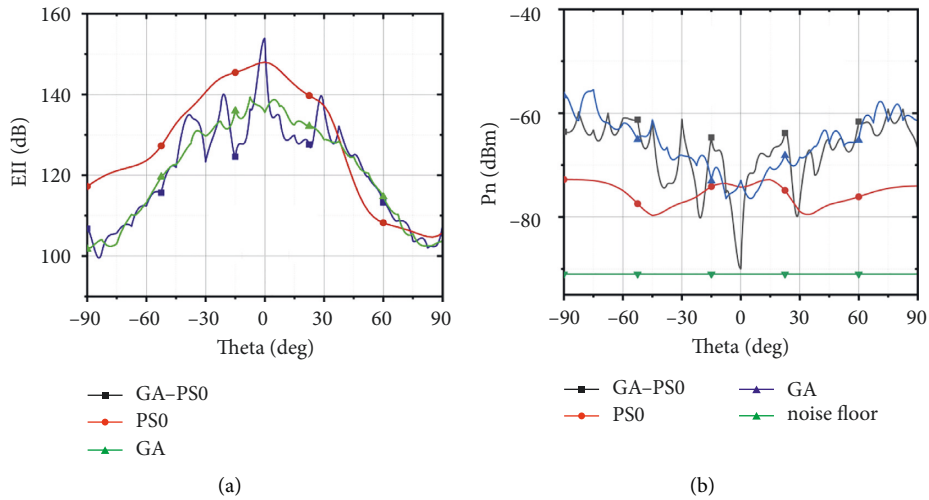

Figure 8: Comparison of performance in three cases at 10 GHz with P_t = 30 W. (a) The EII at three structures. (b) The P_n at three structures.

joint optimization of array aperture and beamforming by GA-PSO obtain the best P_n value (−89.97 dBm) at 0°. P_n obtained by GA-PSO jointly optimized aperture and beamforming is 15.7 dBm lower than GA-optimized transmitting and receiving aperture and 17.1 dBm lower than PSO optimized beamforming. The experimental results show that higher isolation and lower noise can be obtained by using the GA-PSO joint optimization method in the ALSTAR array. The experimental results verify the correctness of the previous array signal model. Therefore, when engineers design the ALSTAR array, its performance can be improved by optimizing the steering vectors and beamforming of the transmit and receive arrays.

5. Conclusions

A hybrid genetic-particle swarm algorithm with combined transmit and receive aperture optimization and beamforming techniques is proposed to enhance isolation in this paper. Specifically, the genetic algorithm is used to optimize the transmit and receive apertures and the particle swarm algorithm is used to optimize the transmit and receive beamforming. Taking the maximum isolation between the transmit and receive apertures as a fitness function, we aim to find the best aperture distribution and transmit and receive beamformers. Besides, the self-interference cancellation model of the ALSTAR array adopts a 1×8 Vivaldi phased array to ensure the authenticity and reliability of the experimental data. The experimental results show that when the transmit power is 30 W, the isolation achieved by only using the aperture optimization technology is 133.27 dB; the isolation achieved by only using the beamforming technology is 147.79 dB, and the isolation achieved by using the combined aperture optimization and beamforming technology is 153.96 dB. Compared with the previous two methods, the scheme in this paper, respectively, improves the isolation of 20.69 dB and 6.17 dB. This shows that combined array aperture optimization and beamforming techniques are effective ways to further improve transmitter and receiver isolation.

Data Availability

No data were used to support this study.

Conflicts of Interest

The authors declare that they have no conflicts of interest.

Acknowledgments

This work was supported by the Guangdong Natural Science Foundation under Grant 2019A1515011622.

References

[1] D. W. Bliss, P. A. Parker, and A. R. Margetts, "Simultaneous transmission and reception for improved wireless network performance," in *Proceedings of the 2007 IEEE/SP 14th Workshop on Statistical Signal Processing*, IEEE, Washington, DC, USA, 2007.

[2] S. Damith Liyanaarachchi, C. Baquero Barneto, T. Riihonen, M. Heino, and M. Valkama, "Joint multi-user communication and MIMO radar through full-duplex hybrid beamforming," in *Proceedings of the 2021 1st IEEE International Online Symposium on Joint Communications & Sensing (JC&S), IEEE*, Germany, 2021.

[3] T. Riihonen, M. Turunen, K. Parlin, M. Heino, J. Marin, and D. Korpi, "Full-duplex operation for electronic protection by detecting communication jamming at transmitter," in *Proceedings of the 2020 IEEE 31st Annual International Symposium on Personal, Indoor and Mobile Radio Communications*, IEEE, London, 2020.

[4] M. Xie, X. Wei, Y. Tang, and D. Hu, "A robust design for aperture-level simultaneous transmit and receive with digital phased array," *Sensors*, vol. 22, no. 1, p. 109, 2021.

[5] T. Riihonen, D. Korpi, O. Rantula, H. Rantanen, T. Valkama, and M. Valkama, "Inband full-duplex radio transceivers: a paradigm shift in tactical communications and electronic warfare?" *IEEE Communications Magazine*, vol. 55, no. 10, pp. 30–36, Oct. 2017.

[6] E. Everett, C. Shepard, L. Sabharwal, and A. Sabharwal, "SoftNull: many-antenna full-duplex wireless via digital beamforming," *IEEE Transactions on Wireless Communications*, vol. 15, no. 12, pp. 8077–8092, 2016.

[7] J. Zhang, S. Li, W. Chang, T. Jiang, B. Li, and Z. Liang, "Study on full-duplex channel characteristic for simultaneous transmit and receive used in phased array," in *Proceedings of the 2019 IEEE International Symposium on Antennas and Propagation and USNC-URSI Radio Science Meeting*, pp. 1495-1496, Georgia, U.S.A, 2019.

[8] J. Zhang, W. Chang, and J. Zheng, "Study on different array allocation for simultaneous transmit and receive used in phased array," in *Proceedings of the 2019 IEEE International Symposium on Phased Array System & Technology (PAST)*, pp. 1–5, Waltham, MA USA, 2019.

[9] J. P. Doane, K. E. Kolodziej, and B. T. Perry, "Simultaneous transmit and receive with digital phased arrays," in *Proceedings of the 2016 IEEE International Symposium on Phased Array Systems and Technology (PAST)*, IEEE, Massachusetts, MA, USA, 2016.

[10] I. T. Cummings, J. P. Doane, T. J. Schulz, and T. C. Havens, "Aperture-level simultaneous transmit and receive with digital phased arrays," *IEEE Transactions on Signal Processing*, vol. 68, pp. 1243–1258, 2020.

[11] C. B. Barneto, S. D. Liyanaarachchi, M. Heino, T. Riihonen, and M. Valkama, "Full duplex radio/radar technology: the enabler for advanced joint communication and sensing," *IEEE Wireless Communications*, vol. 28, no. 1, pp. 82–88, 2021.

[12] H. Lebret and S. Boyd, "Antenna array pattern synthesis via convex optimization," *IEEE Transactions on Signal Processing*, vol. 45, no. 3, pp. 526–532, 1997.

[13] O. Quevedo-Teruel and E. Rajo-Iglesias, "Ant colony optimization in thinned array synthesis with minimum sidelobe level," *IEEE Antennas and Wireless Propagation Letters*, vol. 5, pp. 349–352, 2006.

[14] V. S. Gangwar, A. K. Singh, E. Thomas, and S. P. Singh, "Side lobe level suppression in a thinned linear antenna array using particle swarm optimization," in *Proceedings of the 2015 International Conference on Applied and Theoretical Computing and Communication Technology (iCATccT)*, IEEE, Karnataka, 2015.

[15] I. T. Cummings, "Optimizing the information-theoretic partitioning of simultaneous transmit and receive phased arrays," in *Proceedings of the 2018 IEEE International Symposium on Antennas and Propagation & USNC/URSI National Radio Science Meeting*, IEEE, Boston, MA, 2018.

[16] I. T. Cummings, T. J. Schulz, T. C. Havens, and J. P. Doane, *Performance Simulation and Optimization of a Simultaneous Transmit and Receive Phased Antenna Array Using Adaptive Beamforming and Genetic Algorithm Techniques*, Open Access Master's Report, Michigan Technological University, 2017.

[17] X. Jiang, M. Xie, J. Wei, K. Wang, and L. Peng, "3D-MIMO beamforming realised by AQPSO algorithm for cylindrical conformal phased array," *IET Microwaves, Antennas & Propagation*, vol. 13, no. 15, pp. 2701–2705, 2019.

[18] K. SubhashiniSubhashini and J. Satapathy, "Development of an enhanced ant lion optimization algorithm and its application in antenna array synthesis," *Applied Soft Computing*, vol. 59, pp. 153–173, 2017.

[19] L. Hou, Y. Liu, X. Ma, Y. Li, S. Na, and M. Jin, "Particle swarm optimization inspired low-complexity beamforming for MmWave massive MIMO systems," in *Proceedings of the 2020 IEEE Wireless Communications and Networking Conference*, pp. 1–6, WCNC, Seoul, Korea South, 2020.